International Journal of Thermophysics, Vol. 15, No. 4, 1994

Viscosity of Nitrous Oxide in the Critical Region

C. Yokoyama,[1,2] M. Takahashi,[1] and S. Takahashi[1]

Received February 25, 1994

The gaseous viscosity of nitrous oxide (N_2O) was measured in the critical region. The experimental temperature range was between 309.650 and 318.150 K and the pressure range was up to 9.6 MPa. The measurements were obtained with an oscillating-disk viscometer, combined with local determination of the density at the position of the oscillating disk, and they have an estimated accuracy of 0.6% for viscosity and 0.5% for gas density. The viscosity of N_2O exhibits an anomalous increase near the critical point. The anomalous increase in viscosity was analyzed with the viscosity equation proposed by Basu and Sengers.

KEY WORDS: critical anomaly; mode-coupling theory; nitrous oxide; viscosity.

1. INTRODUCTION

Near a critical point, the viscosity of a fluid exhibits an anomalous increase. Such a critical anomaly behavior has been investigated theoretically and experimentally. In accordance with the practical importance of supercritical fluid technology in the last two decades, the studies on transport properties of near critical and supercritical fluids have significantly increased. To develop and/or examine theoretical models for the critical anomaly of the transport properties, we need accurate data of the transport properties of fluids in the critical region. However, accurate experimental data of viscosity are very scarce because of experimental difficulties. Investigations of the viscosity of fluids in the critical region have been made by several investigators. The viscosity near the critical point has been investigated for various gases such as carbon dioxide [1–7], ethane [5, 8], ethylene [9], xenon [7, 8], hydrogen [10], nitrogen [11], sulfur hexafluoride [12], and water [13].

[1] Research Institute for Chemical Reaction Science, Tohoku University, Sendai 980, Japan.
[2] To whom correspondence should be addressed.

0195-928X/94/0700-0603$07.00/0

Iwasaki and Takahashi [14, 15] developed an oscillating-disk viscometer which can be used to measure the viscosity of fluids near the critical region. The high-pressure chemistry laboratory in Tohoku University has been investigating not only the gas viscosity near the critical point [5, 9], but also both superheated gas and saturated liquid viscosities of various kinds of compounds [16–22]. The present paper describes the continuing work on the experimental determination of viscosity of fluids in the critical region. Here we measured the viscosity of nitrous oxide (N_2O) in the critical region.

The viscosity of gaseous N_2O at normal pressure has been measured by Fisher [23], Trautz and Kurz [24], Trautz and Ruf [25], Johnston and Weimer [26], Johnston and McClosky [27], Raw and Ellis [28], Ellis and Raw [29], Uchiyama [30], Chakraborti and Gray [31], Kerstin and Wakeham [32], Harris et al. [33], Clifford et al. [34], and Kestin and Ro [35], and that of gaseous N_2O under high pressure by Schlumpf et al. [36]. The viscosity of N_2O in the critical region has not been measured yet.

The viscosity equation of N_2O at low densities was studied by Boushehri et al. [37] and Millat et al. [38].

2. EXPERIMENTS

The viscosity was measured with an oscillating-disk viscometer and the density was measured with a high-pressure gas pipette. The characteristics of the suspension system are listed in Table I. The experimental apparatus and procedure are principally the same as those described in previous papers [5, 19, 39, 40]. Therefore, the details of the apparatus and procedure are not presented in this paper. A photodiode and a personal computer were used to obtain the amplitude of the damped oscillations.

Table I. Characteristics of the Suspension System at 298.15 K

Radius of the oscillating disk	14.062 mm
Thickness of the oscillating disk	0.959 mm
Distance between the two fixed disk	1.732 mm
Distance between the oscillating disk and the upper fixed disk	0.386 mm
Distance between the oscillating disk and the lower fixed disk	0.386 mm
Moment of inertia	460.57 g · mm^2
Length of the torsion wire	200 mm
Diameter of the torsion wire	2.0×10^{-2} mm
Period of oscillation in vacuo at 298.15 K	16.199 s
Logarithmic decrement in vacuo at 298.15 K	1.4741×10^{-5} s

The method for calculating the amplitude was the same as that proposed by Ejima et al. [41]. Thus, depending on the rate of damping, 10 to 15 values of the decrement were obtained during each run and averaged. In addition, there complete runs were made at each particular experimental point (given gas, temperature, and pressure) and then averaged. Ten oscillations were analyzed to obtain the amplitude and interval for each single oscillation. The amplitude and interval of the actual damped oscillation were defined as the average of these 10 oscillations. The root mean deviations of the amplitude and interval were about 2×10^{-4} and 1.5×10^{-2}, respectively.

The results of the measurements were evaluated with the aid of Newell's theory [42] in a manner similar to that used by Iwasaki and Kestin [43]. The viscosity was given by the following equation:

$$\eta = 2\pi\rho h^2/\beta^2 T_0 \tag{1}$$

where η represents the viscosity, ρ the density, h the harmonic mean of the distances between the oscillating disk and the upper and/or lower fixed disks, and T_0 the period of oscillation in vacuo. On the other hand, β^2 was

Table II. Calibration of the Edge Correction Factor, C_N, Using Nitrogen as Standard

P (MPa)	ρ (kg·m^{-3})	T (s)	100Δ (μPa·s)	η (μPa·s)	δ (cm)	C_N
Temp. = 298.150 K, R = 14.062 mm, h = 0.388 mm, $I = 4.6057 \times 10^{-7}$ kg·m^2, T_0 = 16.1992 s, $\Delta_0 = 1.4741 \times 10^{-5}$ s						
0.1020	1.153	16.1996	1.7826	17.874	0.63220	1.1237
1.2133	13.741	16.2062	1.7983	18.055	0.18406	1.1221
2.4007	27.226	16.2122	1.8139	18.266	0.13152	1.1188
3.6435	41.350	16.2194	1.8381	18.507	0.10742	1.1188
4.8157	54.654	16.2259	1.8638	18.753	0.09405	1.1194
6.0471	68.579	16.2329	1.8946	19.028	0.08458	1.1212
7.2222	81.791	16.2385	1.9217	19.307	0.07801	1.1205
8.2087	92.805	16.2454	1.9517	19.553	0.07370	1.1234
Ave.						1.1210
Temp. = 323.150 K, R = 14.066 mm, h = 0.388 mm, $I = 4.6096 \times 10^{-7}$ kg·m^2, T_0 = 16.1841 s, $\Delta_0 = 1.5537 \times 10^{-5}$ s						
0.1017	1.061	16.1841	1.8916	18.9574	0.67840	1.1249
1.2764	13.306	16.1914	1.9106	19.1076	0.19232	1.1271
2.4551	25.579	16.1969	1.9251	19.2777	0.13933	1.1257
3.6632	38.121	16.2033	1.9435	19.4715	0.11470	1.1250

Table II. *(Continued)*

P (MPa)	ρ (kg·m^{-3})	T (s)	$100J$ (μPa·s)	η (μPa·s)	δ (cm)	C_N
4.8471	50.357	16.2079	1.9654	19.6797	0.10033	1.1256
5.9838	62.035	16.2139	1.9884	19.8958	0.09089	1.1262
7.2170	74.605	16.2206	2.0169	20.1472	0.08340	1.1279
8.3411	85.956	16.2253	2.0427	20.3909	0.07817	1.1285
Ave.						1.1264
Temp. = 348.150 K, R = 14.074 mm, h = 0.388 mm, $I = 4.6136 \times 10^{-7}$ kg·m^2, T_0 = 16.1681 s, $J_0 = 2.4414 \times 10^{-5}$ s						
0.1017	0.984	16.1691	2.0123	20.0488	0.72408	1.1315
1.2308	11.892	16.1749	2.0250	20.1815	0.20897	1.1322
2.3253	22.426	16.1804	2.0374	20.3244	0.15271	1.1301
3.5596	34.245	16.1851	2.0554	20.5017	0.12412	1.1303
4.8105	46.142	16.1918	2.0760	20.6981	0.10744	1.1306
6.0398	57.738	16.1976	2.0966	20.9066	0.09653	1.1303
7.3697	70.161	16.2029	2.1205	21.1484	0.08807	1.1300
8.7258	82.677	16.2088	2.1496	21.4112	0.08163	1.1312
Ave.						1.1308
Temp. = 373.150 K, R = 14.080 mm, h = 0.388 mm, $I = 4.6157 \times 10^{-7}$ kg·m^2, T_0 = 16.1563 s, $J_0 = 4.0875 \times 10^{-5}$ s						
0.1014	0.916	16.1572	2.1347	21.1050	0.76971	1.1399
1.1811	10.636	16.1613	2.1473	21.2225	0.22651	1.1404
2.3277	20.903	16.1680	2.1598	21.3599	0.16210	1.1395
3.4716	31.077	16.1717	2.1754	21.5095	0.13341	1.1398
4.6738	41.687	16.1784	2.1904	21.6795	0.11564	1.1385
5.9389	52.749	16.1820	2.2106	21.7190	0.10290	1.1469
7.1806	63.493	16.1876	2.2270	22.0733	0.09455	1.1368
8.5344	75.068	16.1917	2.2518	22.3062	0.08741	1.1374
Ave.						1.1399
Temp. = 398.150 K, R = 14.086 mm, h = 0.388 mm, $I = 4.6215 \times 10^{-7}$ kg·m^2, T_0 = 16.1460 s, $J_0 = 6.8298 \times 10^{-5}$ s						
0.1015	0.858	16.1465	2.2336	22.1297	0.81412	1.1364
1.1213	9.459	16.1507	2.2521	22.2329	0.24576	1.1406
2.3351	19.624	16.1564	2.2592	22.3674	0.17114	1.1372
3.5916	30.058	16.1595	2.2741	22.5192	0.13875	1.1372
4.8130	40.106	16.1653	2.2884	22.6786	0.12054	1.1362
6.0020	49.792	16.1719	2.3067	22.8443	0.10858	1.1367
7.1679	59.189	16.1743	2.3197	23.0162	0.09996	1.1347
8.3777	68.832	16.1791	2.3423	23.2040	0.09307	1.1364
Ave.						1.1369

determined from the measured values of the logarithmic decrement Δ and period of oscillation T from the cubic equation

$$C_N = \left[\frac{2I}{\pi\rho b R^4}\left(\frac{\Delta}{\tau} - \Delta_0\right) + a\frac{\Delta}{\tau}\right]\beta^2 + f\frac{\Delta^2 - 1}{\tau^2}\beta^4 + h\frac{\Delta(\Delta^2 - 1)}{\tau^3}\beta^6 \quad (2)$$

where $a = 2/3$, $f = 1/45$, and $h = 8/945$, if $b_1 = b_2$. It was confirmed that the present measurements satisfactorily fulfill the condition on which Eqs. (1) and (2) will yield the required accuracy of 0.1 %.

The edge-correction factor C_N was obtained using nitrogen as a standard. The viscosity data of nitrogen were taken from Stephan et al. [44] and the density data were obtained from the equation of state proposed by Jacobsen and Stewart [45]. The results for the calibration of the viscometer are shown in Table II. It can be seen that the C_N shows a temperature dependency, while the pressure dependency can be ignored. The values of C_N as a function of temperature are shown in Fig. 1. The C_N can be deduced in the form of simple polynomials of temperature as follows:

$$C_N = 0.90161 + 1.1466 \times 10^{-3} T - 1.3864 \times 10^{-6} T^2 \quad (3)$$

where T is the temperature in K.

The pressure of the sample was measured with a mercury U-tube detector and a deadweight gauge. The accuracy of the measurements of the pressure is estimated to be 10 kPa. The temperature of the thermostat was measured with a quartz thermometer calibrated against a Leed–Northrup platinum resistance thermometer and was kept constant to about

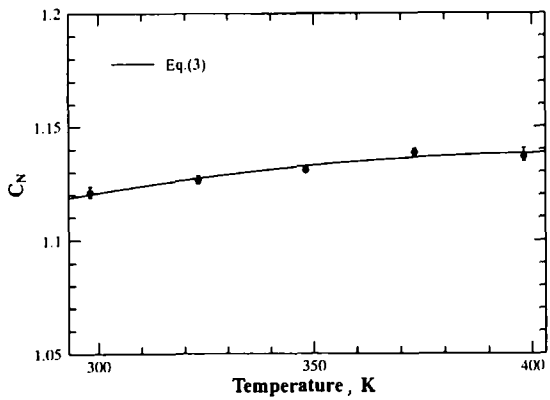

Fig. 1. Edge correction factor C_N as a function of temperature.

± 0.003 K over the period of the measurements. The temperature of the viscometer was kept to within 0.001 K. The accuracy of the temperature measurements is estimated to be ± 0.003 K. The accuracy of the density measurements is estimated to be 0.4%. The accuracy of the present viscosity measurements is at worst ± 0.6% considering the uncertainties in the determination of the logarithmic decrement, the period of oscillation, the density of the gas, and other sources of error.

The N_2O was obtained from Seitetsu-Kagaku Co., with a stated purity better than 99.999 mol%, and was used in this experiment without further purification.

3. RESULTS AND DISCUSSION

The experimental results are presented in Table III and shown in Figs. 2–4. Table IV shows a comparison of the present data for the viscosity at

Table III. Viscosity of Nitrous Oxide

P (MPa)	ρ (kg·m^{-3})	η (μPa·s)
	$T = 309.650$ K	
0.1020	1.752	15.442
0.1045	1.795	15.450
0.3881	6.760	15.450
0.7007	12.397	15.488
1.1911	21.620	15.554
1.6819	31.358	15.619
2.1559	41.659	15.781
2.6709	52.865	15.891
3.2254	66.442	16.091
3.7469	80.596	16.314
4.2360	95.130	16.593
4.7026	110.63	16.896
5.0488	123.01	17.185
5.3562	136.44	17.473
5.7290	153.90	17.925
6.0750	173.11	18.496
6.3662	192.81	19.100
6.6083	213.11	19.770
6.7965	233.14	20.492
6.9371	252.63	21.233
7.0313	269.56	21.963
7.1075	287.91	22.783
7.1515	302.24	23.490
7.1849	316.62	24.158

Table III. *(Continued)*

P (MPa)	ρ (kg · m^{-3})	η (μPa · s)
7.1870	317.54	24.246
7.2119	333.64	25.138
7.2239	344.50	25.748
7.2322	354.70	26.403
7.2386	364.26	27.051
7.2420	371.99	27.555
7.2445	378.51	27.890
7.2457	385.80	28.588
7.2469	391.76	29.048
7.2481	398.64	29.649
7.2487	406.24	30.196
7.2495	407.41	30.408
7.2510	416.81	31.062
7.2516	430.55	32.147
7.2517	441.25	33.208
7.2521	449.62	34.201
7.2522	459.89	35.516
7.2523	471.39	35.541
7.2525	476.58	35.814
7.2534	488.09	36.549
7.2537	490.40	36.372
7.2539	495.18	36.601
7.2545	501.65	36.905
7.2555	507.61	37.290
7.2570	513.22	37.578
7.2601	521.55	38.127
7.2643	528.34	38.548
7.2686	535.75	39.036
7.2750	543.31	39.599
7.2829	550.73	40.129
7.2944	554.56	40.586
7.3071	562.62	41.281
7.3239	570.33	41.967
7.3464	577.47	42.588
7.3742	586.79	43.301
7.4086	595.23	44.016
7.4514	604.80	44.835
	$T = 309.750$ K	
0.1032	1.772	15.449
0.3486	6.058	15.455
0.5968	10.500	15.485

Table III. *(Continued)*

P (MPa)	ρ (kg · m^{-3})	η (μPa · s)
1.1278	20.397	15.547
1.6165	30.020	15.629
2.1156	40.428	15.740
2.5570	50.217	15.844
3.1123	63.524	16.036
3.5716	75.575	16.229
4.1000	90.855	16.494
4.6084	107.30	16.825
5.0004	121.98	17.143
5.2555	131.85	17.391
5.5605	145.50	17.720
5.8439	159.68	18.119
6.1127	175.16	18.568
6.3147	188.54	18.939
6.5080	203.54	19.443
6.6719	218.62	19.964
6.8115	234.09	20.532
6.9253	24'9.37	21.156
7.0192	265.19	21.777
7.0843	279.44	22.416
7.1356	293.21	23.054
7.1736	306.58	23.716
7.1993	318.40	24.311
7.2169	328.41	24.847
7.2313	337.93	25.478
7.2408	349.46	26.100
7.2470	357.02	26.536
7.2518	364.44	27.088
7.2552	372.02	27.559
7.2581	380.16	28.070
7.2599	387.29	28.633
7.2617	395.14	29.195
7.2631	402.87	29.773
7.2634	410.79	30.428
7.2645	418.63	31.108
7.2648	425.77	31.789
7.2652	432.91	32.481
7.2658	440.36	33.147
7.2663	449.16	33.734
7.2691	453.31	34.136
7.2694	459.15	34.565
7.2695	465.95	34.957
7.2703	471.27	35.239

Table III. *(Continued)*

P (MPa)	ρ (kg · m^{-3})	η (μPa · s)
7.2707	476.52	35.512
7.2713	482.31	35.813
7.2728	487.34	36.068
7.2732	492.58	36.354
7.2738	498.22	36.669
7.2759	504.87	36.966
7.2785	511.97	37.396
7.2812	518.55	37.878
7.2854	525.90	38.363
7.2901	533.29	38.925
7.2966	540.84	39.426
7.3054	548.82	39.961
7.3156	555.91	40.597
7.3311	564.24	41.232
7.3499	572.31	41.922
7.3717	580.97	42.619
7.3995	588.73	43.363
7.4356	596.40	44.177
7.4778	604.82	44.948
	$T = 309.850$ K	
0.1011	1.736	15.429
0.5958	10.478	15.486
1.0990	19.838	15.572
1.6539	30.768	15.661
2.1773	41.738	15.755
2.6390	52.070	15.793
3.1887	65.491	16.085
3.7433	80.290	16.319
4.2671	95.888	16.612
4.6999	110.34	16.894
5.3212	134.49	17.454
5.9115	162.91	18.198
6.3089	187.97	18.954
6.5892	210.52	19.662
6.7848	229.86	20.368
6.9615	253.22	21.262
7.0721	273.48	22.165
7.1354	289.05	22.855
7.1881	306.42	23.704
7.2266	324.98	24.669
7.2514	342.13	25.687

Table III. *(Continued)*

P (MPa)	ρ (kg·m^{-3})	η (μPa·s)
7.2621	353.55	26.262
7.2698	364.97	26.940
7.2762	378.00	27.960
7.2806	391.05	28.548
7.2832	404.56	29.429
7.2857	416.04	30.402
7.2887	434.32	31.471
7.2898	445.03	32.458
7.2909	458.25	33.431
7.2914	467.96	34.349
7.2925	476.32	34.910
7.2934	485.63	35.477
7.2957	492.55	35.897
7.2975	500.36	36.445
7.2990	508.01	37.009
7.3021	515.51	37.504
7.3058	523.50	38.005
7.3122	532.02	38.744
	$T = 310.150$ K	
0.1022	1.753	15.471
0.2999	5.194	15.483
0.6900	12.181	15.529
1.0797	19.442	15.552
1.5711	29.040	15.646
2.0527	38.989	15.746
2.5165	49.164	15.879
3.0863	62.742	16.051
3.6014	76.298	16.262
4.0456	88.860	16.467
4.6397	108.05	16.877
5.2853	132.35	17.429
5.7673	154.55	17.993
6.0966	172.77	18.495
6.3660	190.65	19.072
6.6902	218.01	19.944
6.9555	248.91	21.155
7.1414	283.44	22.643
7.2073	302.83	23.565
7.2492	320.55	24.447
7.2785	337.53	25.330
7.2972	353.97	26.313

Table III. *(Continued)*

P (MPa)	ρ (kg·m^{-3})	η (μPa·s)
7.3071	365.65	27.005
7.3134	377.53	27.586
7.3186	389.38	28.470
7.3228	400.54	29.247
7.3258	413.56	30.134
7.3287	424.90	30.903
7.3292	434.61	31.674
7.3312	446.69	32.567
7.3344	456.93	33.395
7.3408	467.08	34.090
7.3409	477.67	34.834
7.3439	487.44	35.512
7.3457	495.76	36.157
7.3563	507.13	36.876
7.3649	519.08	37.712
7.3742	530.96	38.560
7.3872	542.36	39.473
7.3978	550.19	40.036
7.4121	556.37	40.658
7.4298	565.70	41.399
7.4511	573.95	42.066
	$T = 311.150$ K	
0.1020	1.744	15.529
0.2959	5.105	15.533
0.5867	10.377	15.555
0.8858	15.742	15.594
1.2866	23.342	15.633
1.7680	32.916	15.729
2.1694	41.321	15.829
2.6502	51.981	15.958
3.1979	65.145	16.149
3.7111	78.531	16.368
4.1687	91.850	16.624
4.6280	106.50	16.898
4.9996	119.88	17.186
5.3558	133.67	17.522
5.7277	150.48	17.959
5.9869	163.75	18.321
6.1874	175.34	18.635
6.5789	202.30	19.502

Table III. *(Continued)*

P (MPa)	ρ (kg·m^{-3})	η (μPa·s)
6.8718	229.23	20.438
7.0752	254.65	21.411
7.2259	281.41	22.570
7.3150	304.54	23.674
7.3653	322.58	24.616
7.4007	339.16	25.468
7.4248	355.40	26.419
7.4381	366.14	27.027
7.4480	376.87	27.676
7.4563	387.22	28.394
7.4643	399.19	29.116
7.4706	410.52	29.829
7.4784	421.33	30.600
7.4833	432.31	31.377
7.4901	444.32	32.135
7.4960	455.92	32.925
7.4996	468.42	33.846
7.5122	479.91	34.716
7.5143	492.66	35.565
7.5230	506.53	36.593
7.5379	520.21	37.607
7.5548	533.09	38.641
7.5849	547.48	39.802
7.6142	560.06	40.895
7.6500	571.21	41.850
7.6898	581.22	42.732
7.7272	589.56	43.465
7.7727	597.88	44.362
7.8293	606.22	45.078
7.8932	614.70	45.970
7.9680	624.04	46.854
	$T = 313.150$ K	
0.1019	1.730	15.627
0.2523	4.316	15.629
0.4377	7.556	15.647
0.6434	11.275	15.671
0.9302	16.446	15.702
1.3330	24.054	15.769
1.7820	32.937	15.846

Table III. *(Continued)*

P (MPa)	ρ (kg·m^{-3})	η (μPa·s)
2.4505	47.051	16.021
3.0881	61.774	16.237
3.6406	75.826	16.443
4.2767	93.923	16.767
4.8108	111.00	17.115
5.2189	125.60	17.461
5.5134	137.41	17.719
5.7786	149.17	18.022
6.0191	160.56	18.344
6.2196	171.18	18.648
6.4249	183.34	19.035
6.6306	196.99	19.428
6.9749	225.02	20.383
7.2114	250.26	21.397
7.3609	271.64	22.345
7.4577	289.02	23.065
7.5480	309.66	24.025
7.6176	330.57	25.057
7.6688	350.73	26.204
7.6972	364.04	26.962
7.7174	376.10	27.597
7.7336	385.49	28.242
7.7490	396.83	28.881
7.7630	406.93	29.580
7.7760	417.65	30.293
7.7878	427.63	30.979
7.8008	439.17	31.721
7.8126	448.80	32.393
7.8244	458.85	33.025
7.8377	469.60	33.796
7.8513	479.88	34.563
7.8672	490.24	35.280
7.8818	499.71	35.988
7.9056	512.89	36.943
7.9475	530.18	38.344
7.9684	537.77	38.984
7.9928	546.89	39.639
8.0453	564.39	40.814
8.1051	573.35	42.043
8.1817	586.26	43.186
8.2381	594.40	43.959
8.3031	603.01	44.714
8.3820	611.71	45.631

Table III. *(Continued)*

P (MPa)	ρ (kg · m^{-3})	η (μPa · s)
8.4687	620.03	46.501
8.5701	626.91	47.385
8.6850	638.19	48.299
	$T = 318.150$ K	
0.1015	1.696	15.881
0.2482	4.176	15.897
0.4033	6.832	15.923
0.6434	11.025	15.943
0.8876	15.384	15.968
1.1798	20.739	16.004
1.1959	26.715	16.050
1.8385	33.421	16.129
2.1809	40.390	16.213
2.5114	47.381	16.286
2.8529	54.921	16.389
3.1895	64.684	16.508
3.5133	70.473	16.626
3.7142	75.187	16.693
4.0377	83.983	16.848
4.3277	91.952	16.998
4.6826	101.14	17.207
4.9372	110.29	17.390
5.2704	121.66	17.645
5.6149	134.01	17.942
5.9582	147.72	18.289
6.2874	161.25	18.680
6.5170	173.91	19.046
6.7286	185.40	19.366
6.9242	196.91	19.742
7.0920	207.84	20.122
7.2558	219.38	20.523
7.4097	231.53	20.988
7.5487	243.75	21.440
7.6718	255.85	21.945
7.8171	269.90	22.489
7.9007	281.53	23.025
7.9913	295.30	23.617
8.0663	307.24	24.180
8.1408	319.81	24.769
8.2035	332.07	25.425
8.2541	341.97	25.970

Table III. *(Continued)*

P (MPa)	ρ (kg·m^{-3})	η (μPa·s)
8.2983	353.65	26.521
8.3398	363.50	27.112
8.3862	373.95	27.688
8.4244	384.78	28.334
8.4626	395.67	28.979
8.5007	407.05	29.674
8.5357	418.60	30.396
8.5703	428.75	31.064
8.6049	440.09	31.760
8.6401	450.89	32.499
8.6785	462.48	33.260
8.7023	471.03	33.729
8.7260	477.00	34.222
8.7495	482.34	34.712
8.7995	495.13	35.660
8.8494	505.84	36.510
8.9083	518.35	37.467
9.0007	535.54	38.898
9.0479	542.52	39.506
9.0984	550.56	40.165
9.1592	558.27	40.796
9.2234	567.30	41.523
9.2917	574.70	42.260
9.3679	582.67	42.966
9.4539	591.22	43.769
9.5459	599.87	44.584

Table IV. Comparison of Viscosity Values of N_2O at Atmospheric Pressure

T (K)	η (μPa·s)		
	This work	Millat et al. [38]	Boushehri et al. [37]
309.65	15.442	15.445	15.500
309.75	15.449	15.450	15.506
309.85	15.459	15.455	15.511
310.15	15.471	15.470	15.526
311.15	15.529	15.521	15.578
313.15	15.627	15.622	15.681
318.15	15.881	15.871	15.938

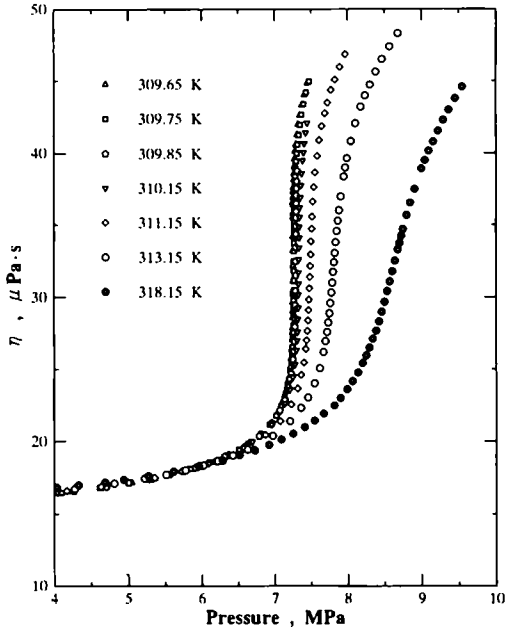

Fig. 2. Viscosity of N_2O as a function of pressure.

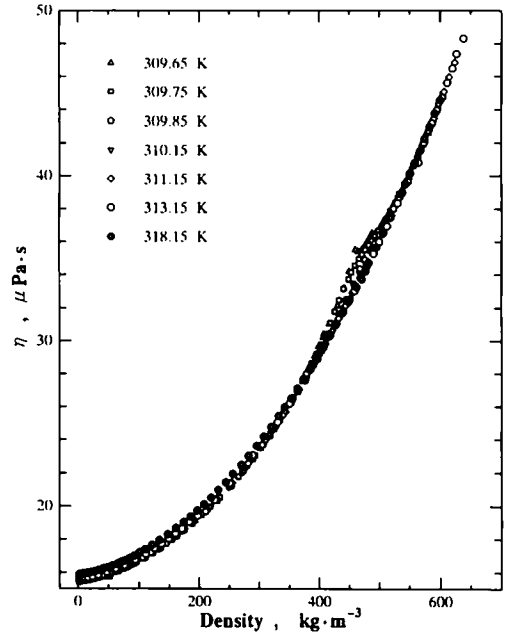

Fig. 3. Viscosity of N_2O as a function of density.

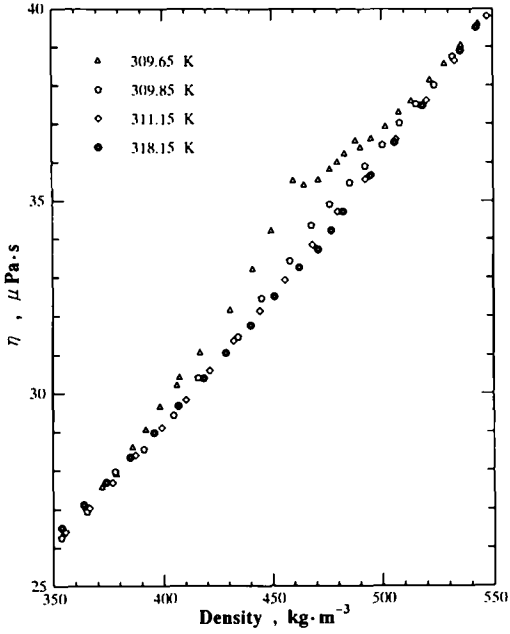

Fig. 4. Viscosity of N_2O in the critical region as a function of density.

normal pressure with those calculated from the viscosity equations proposed by Boushehri et al. [37] and Millat et al. [38]. The present data agree extremely well with those calculated from the equation of Millat et al., while the values calculated from the equation of Boushehri et al. deviate about 0.35% from the present data. Figure 2 shows a plot of the viscosity against the pressure. The viscosity increases rapidly near the critical point. In Figs. 3 and 4, the viscosity is plotted against the density for the same temperatures. Figure 4 represent in more detail the critical region. It can be seen from Figs. 3 and 4 that the viscosity indicates an anomalous increase near the critical point. The present results may be the first to show the critical anomaly of the viscosity of N_2O.

To represent the anomalous behavior of the viscosity in the critical region, it is necessary to know the behavior of a background viscosity [46–48]. As suggested by Sengers [46], the experimental viscosity $\eta(\rho, T)$ can be separated into an anomalous part $\Delta\eta(\rho, T)$ and a background viscosity $\bar{\eta}(\rho, T)$, i.e.,

$$\eta(\rho, T) = \bar{\eta}(\rho, T) + \Delta\eta(\rho, T) \tag{4}$$

The background viscosity is obtained empirically by extrapolating the behavior of the viscosity outside the critical region, and it may be written as

$$\bar{\eta}(\rho, T) = \eta_0(T) + \eta_e(\rho, T) \tag{5}$$

where $\eta_0(T)$ is the viscosity in the limit of low densities and $\eta_e(\rho, T)$ is the excess viscosity. In this study $\eta_0(T)$ was assumed to be the viscosity at atmospheric pressure. The excess viscosity is defined as follows:

$$\eta_e(\rho, T) = \bar{\eta}(\rho, T) - \eta_0(T) \tag{6}$$

and is for many gases a function of density along, $\eta_e(\rho, T) \approx \eta_e(\rho)$, to a good approximation at high temperatures above the critical one. In this study the excess viscosity was evaluated from the data at 318.15 K and was represented by a simple polynomial in the density:

$$\begin{aligned}\eta_e(\rho) &= \bar{\eta}(\rho, T) - \eta_0(T) \\ &= a_1\rho_e + a_2\rho_e^2 + a_3\rho_e^3 + a_4\rho_e^4 + a_5\rho_e^5\end{aligned} \tag{7}$$

where η is in μPa·s and ρ_e is an excess density in kg m^{-3} defined as

$$\rho_e = \rho - \rho_0 \tag{8}$$

where ρ_0 is the density at atmospheric pressure. In Eq. (7), a_i are constants with the values $a_1 = 5.90466 \times 10^{-3}$, $a_2 = 7.04603 \times 10^{-5}$, $a_3 = 1.75193 \times 10^{-8}$, $a_4 = -9.63621 \times 10^{-11}$, and $a_5 = 1.12491 \times 10^{-13}$.

The measured viscosity $\eta(\rho, T)$ at 318.15 K can be reproduced by Eq. (7) and $\eta_0(T)$ with a deviation not exceeding the experimental error. Since $\eta_e(\rho)$ is established as a function of the density ρ, the background viscosity $\bar{\eta}(\rho, T)$ can be obtained from Eq. (6). Then the anomalous viscosity $\Delta\eta$ can be obtained from the experimental viscosity and the background viscosity by Eq. (5). The empirical values thus obtained for $\Delta\eta$ are shown in Fig. 5. As can be seen, the $\Delta\eta$ have a maximum near the critical density.

Close to the critical region, a simplified theoretical treatment based on the mode-coupling theory yields the following power law [49, 50]:

$$\eta/\bar{\eta} = (q\xi)^{\phi} \tag{9}$$

where q is a constant, ξ is the correlation length, and ϕ is an universal exponent. The original estimate for the value of ϕ from the mode-coupling theory is $8/15\pi^2 = 0.054$. Recently, this has been shown to be inconsistent with most experimental data for the critical enhancement of the viscosity

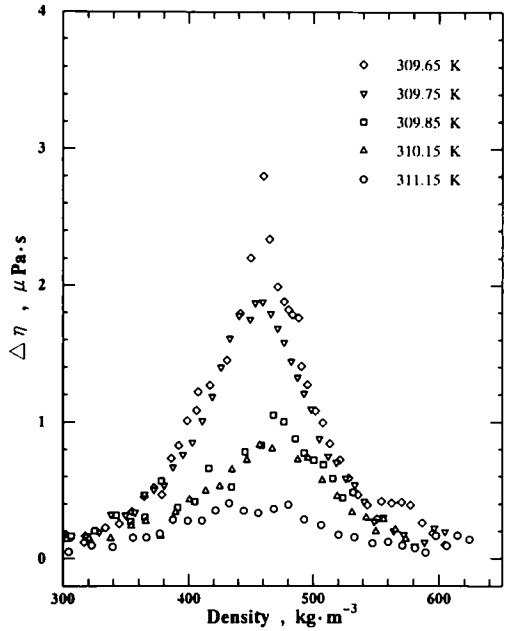

Fig. 5. Anomalous viscosity $\Delta\eta$ of N_2O.

and should be replaced by a value closer to 0.065 [51–53]. In this study, therefore, we used the value of 0.065 for ϕ. Sengers et al. [47] suggested that Eq. (9) can be rewritten in terms of the symmetrized isothermal compressibility as follows:

$$\begin{aligned} \eta/\bar{\eta} &= (\chi_T^*/\chi_0^*)^{\nu\phi/\gamma} \quad \text{for} \quad \chi_T^* > \chi_0^* \\ \eta/\bar{\eta} &= 1 \quad \text{for} \quad \chi_T^* < \chi_0^* \end{aligned} \tag{10}$$

where χ_T^* is a reduced symmetrized compressibility, $\chi_0^* = \Gamma/(q\xi_0)^{2-\eta}$, γ, ν are critical exponents, Γ is the critical amplitude of χ_T^*, and ξ_0 is the critical amplitude of ξ. Equations (9) and (10) are useful for the correlation of viscosity data in the critical region.

According to the mathematical relationships derived by Levelt Sengers et al. [54] and Basu and Sengers [55], χ_T^*, ξ_0, and ξ were calculated with the use of the linear model scaled equation of state for N_2O proposed by Ohgaki et al. [56]. The calculated values with the scaled equation of state and the present data for the $P\rho T$ relationships in the critical region were compared and the result is shown in Fig. 6. It can be seen that the present data for the $P\rho T$ relationships are consistent with the scaled equation of

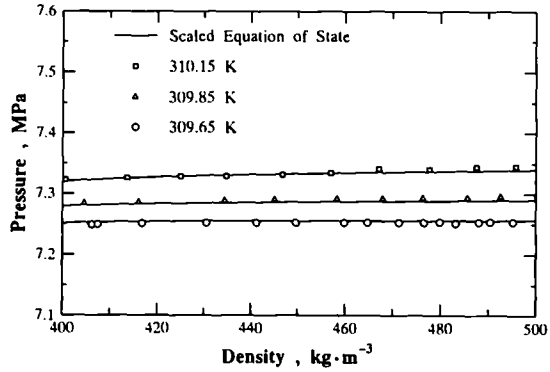

Fig. 6. $P\rho T$ relationships of N_2O in the critical region.

Ohgaki et al. Based on this agrteement for the $P\rho T$ relationships, we decided to use the values of the critical parameters, T_C, ρ_C, and P_C, determined by Ohgaki et al. [56] in the following analysis of critical anomaly.

The values of ϕ and q can be determined from the double logaritmic plot of the viscosity ratio $\eta/\bar{\eta}$ and the ξ as suggested by Basu and Sengers. Figure 6 shows the double logarithmic plot. As suggested by Basu and Sengers, it can be seen that at high values of ξ the data follow a straight line, whose slope yields the effective exponent ϕ and whose intercept on the ξ axis yields q^{-1}. However, the values of ϕ and q^{-1} could not be determined unconditionally with a least-squares fitting of the double logarithmic plot, partly because of the scatter of the data and partly because of the low magnitude of the critical anomaly of N_2O compared with the case of N_2.

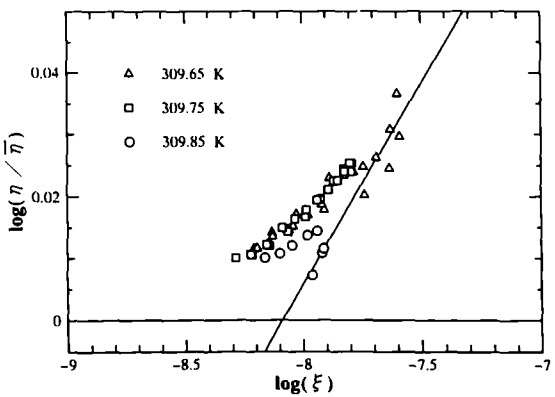

Fig. 7. A double logarithmic plot of the viscosity ratio as a function of the correlation length.

Table V. Critical-Region Parameters for Nitrous Oxide

Critical parameters
$T_C = 309.56$ K
$P_C = 7.238 \times 10^6$ Pa
$\rho_C = 453.3$ kg · m $^{-3}$
Critical exponents
$\beta = 0.355$
$\gamma = 1.190$
$\nu = 0.633$
Correlation length scale factor
$\xi_0 = 1.5 \times 10^{-10}$ m

Therefore, in this study, the value of ϕ was fixed to the value 0.065, and the value of q^{-1} was obtained from the data at three isotherms of 309.65, 309.75, and 309.85 K and in the density range of 390–510 kg · m^{-3} (309.65 K), 390–520 kg · m^{-3} (309.75 K), and 430–510 kg · m^{-3} (309.85 K). The value obtained was $q^{-1} = 81 \times 10^{-10}$ m.

Table V shows the critical parameters used in this study. According to Eq. (8), the viscosity can be calculated with the results of q, ϕ, and the compressibility. The comparison between the calculated results and the experimental data at 309.650 and 318.150 K is shown in Fig. 7.

Recently, Olchowy and Sengers [57] proposed a crossover viscosity equation that can incorporate the crossover from the singular behavior of

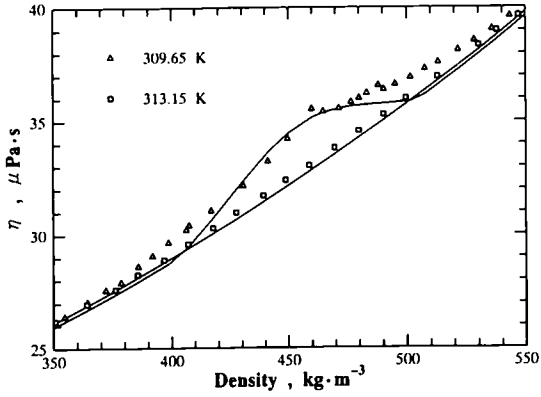

Fig. 8. Comparison between the calculated valuers and the experimental viscosity at 309.650 and 318.150 K.

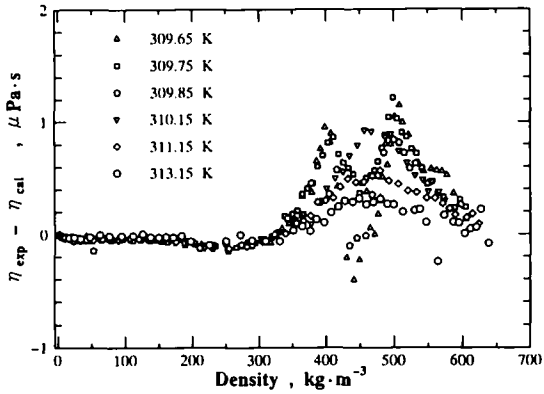

Fig. 9. Deviations of the experimental viscosity values of N_2O from those calculated with Eq. (4).

the viscosity asymptotically close to the critical point to the nonsingular background behavior far away from the critical point. To apply the crossover equation to the present results, we need a scaled fundamental equation for the thermodynamic properties, e.g., density and isothermal and isobaric heat capacities, of N_2O in the critical region. However, surprisingly few studies have ever tried to derive the scaled equation for N_2O. While Ohgaki et al. proposed the scaled equation of state for N_2O based on a linear model, they used the $P\rho T$ data only to determine the parameters of the scaled equation. It should be necessary to refine the scaled equation using data of the specific heat of N_2O. Additional experimental information not only for the viscosity but also for other thermophysical properties, including the thermal conductivity, of N_2O in the critical region is required to analyze the critical viscosity anomaly of N_2O with the theory of dynamic critical phenomena.

4. CONCLUSION

We made highly accurate and precise measurements of the gas viscosity for N_2O in the critical region with the use of the oscillating-disk viscometer. The critical anomaly could be observed at the viscosity isotherms at 309.650, 309.750, and 309.850 K. The viscosity equation derived from the mode-coupling theory was applied to fit the experimental data. It was found that the our data obeyed the viscosity equation from the mode-coupling theory.

ACKNOWLEDGMENTS

The authors are indebted to Emeritus Professor Hiroji Iwasaki for his encouragement. This work was founded by Grant-in-Aid for Scientific Research 04238102 from the Ministry of Education, Science, and Culture of Japan, which is gratefully acknowledged.

REFERENCES

1. S. N. Naldrett and O. Maass, *Can. J. Res.* **18B**:322 (1940).
2. A. Michels, A. Botzen, and W. Schuurman, *Physica* **23**:95 (1957).
3. J. Kestin, J. H. Whitelaw, and T. F. Zien, *Physica* **30**:161 (1964).
4. W. Herreman, A. Laattenist, W. Grevendonk, and A. De Bock, *Physics* **52**:489 (1971).
5. H. Iwasaki and M. Takahashi, *J. Chem. Phys.* **74**:1930 (1981).
6. L. Bruschi and G. Torzo, *Phys. Lett.* **98A**:265 (1983).
7. R. F. Berg and M. R. Moldover, *J. Chem. Phys.* **93**:1926 (1990).
8. H. J. Strumpf, A. F. Collings, and C. J. Pings, *J. Chem. Phys.* **60**:1309 (1974).
9. H. Iwasaki and M. Takahashi, in *Proceedings of the 4th International Conference on High Pressure*, Kyoto (1974), p. 523.
10. D. E. Diller, *J. Chem. Phys.* **42**:2089 (1965).
11. V. N. Zozulya and Yu. P. Blagoi, *Sov. Phys. JETP* **39**:99 (1974).
12. J. H. B. Hoogland and N. J. Trappeniers, in *Proceedings of the 8th Symposium on Thermophysical Properties*, J. V. Sengers, ed. (American Society of Mechanical Engineers, New York, 1982), Vol. I, p. 440.
13. S. L. Rivkin, A. Ja. Levin, L. B. Izrailevsky, and K. G. Kharitonov, in *Proceedings of the 8th International Conference on the Properties of Water and Steam*, Paris (1975), p. 153.
14. H. Iwasaki and H. Takahashi, *Bull. Chem. Res. Inst. Non-Aqueous Solut. Tohoku Univ.* **6**:61 (1956).
15. H. Iwasaki and M. Takahashi, *Rev. Phys. Chem. Jpn.* **38**:18 (1968).
16. M. Takahashi, S. Takahashi, and H. Iwasaki, *J. Chem. Eng. Data* **30**:10 (1985).
17. M. Takahashi, C. Yokoyama, and S. Takahashi, *J. Chem. Eng. Data* **32**:98 (1987).
18. M. Takahashi, C. Yokoyama, and S. Takahashi, *Int. Chem. Eng.* **27**:85 (1987).
19. M. Takahashi, C. Yokoyama, and S. Takahashi, *J. Chem. Eng. Eng. Data* **33**:267 (1988).
20. M. Hongo, C. Yokoyama, and S. Takahashi, *J. Chem. Eng. Jpn.* **21**:632 (1988).
21. A. Kumagai and S. Takahashi, *Int. J. Thermophys.* **12**:105 (1991).
22. A. Kumagai, H. Mochida, and S. Takahashi, *Int. J. Thermophys.* **14**:45 (1993).
23. W. Fisher, *Phys. Rev.* **28**:73 (1909).
24. M. Trautz and F. Kurz, *Ann. Phys.* **9**:981 (1931).
25. M. Trautz and F. Ruf, *Ann. Phys.* **20**:127 (1934).
26. H. L. Johnston and H. R. Weimer, *J. Am. Chem. Soc.* **56**:625 (1934).
27. H. L. Johnston and K. E. McClosky, *J. Phys. Chem.* **44**:1038 (1940).
28. C. J. G. Raw and C. P. Ellis, *J. Chem. Phys.* **28**:1198 (1958).
29. C. P. Ellis and C. J. G. Raw, *J. Chem. Phys.* **30**:574 (1959).
30. H. Uchiyama, *Chem. Eng. Jpn.* **19**:342 (1965).
31. P. K. Chakraborti and P. Gray, *Trans. Faraday Soc.* **61**:2422 (1965).
32. J. Kestin and W. A. Wakeham, *Ber. Bunsenges. Phys. Chem.* **83**:573 (1979).
33. E. J. Harris, G. C. Hope, D. W. Gough, and E. B. Smith, *J. Chem. Soc. Faraday Trans. I* **75**:892 (1979).
34. A. A. Clifford, P. Gray, and A. C. Scott, *J. Chem. Soc. Faraday Trans. I* 77:892 (1979).

35. J. Kestin and S. T. Ro, *Ber. Bunsenges. Phys. Chem.* **86**:948 (1982).
36. J. P. Schlumpf, F. Lazarre, and P. Vaillet, *J. Chim. Phys.* **72**:631 (1975).
37. A. Boushedri, J. Bzowski, J. Kestin, and E. A. Mason, *J. Phys. Chem. Ref. Data* **16**:455 (1987); Erratum, *J. Phys. Chem. Ref. Data* **17**:255 (1988).
38. J. Millat, V. Vesovic, and W. A. Wakeham, *Int. J. Thermophys.* **12**:265 (1991).
39. M. Takahashi, C. Yokoyama, and S. Takahashi, *Trans. JAR* **4**:25 (1987).
40. M. Takahashi, C. Yokoyama, and S. Takahashi, *Trans. JAR* **6**:57 (1989).
41. T. Ejima, Y. Sato, S. Yaegashi, T. Kijima, E. Takeuchi, and K. Tamai, *Nippon Kinzoku Gakkaishi* **51**:328 (1987).
42. G. F. Newell, *J. Appl. Math. Phys.* **10**:160 (1959).
43. H. Iwasaki and J. Kestin, *Physica* **29**:1345 (1963).
44. K. Stephan, R. Krauss, and A. Laesecke, *J. Phys. Chem. Ref. Data* **16**:993 (1987).
45. R. T. Jacobsen and R. B. Stewart, *J. Phys. Chem. Ref. Data* **2**:757 (1973).
46. J. V. Sengers, in *Proceedings of the International School of Physics, "Enrico Fermi," Course 51, "Critical Phenomena,"* M. S. Green, ed. (1971), p. 445.
47. J. V. Sengers, in *Transport Phenomena—1973*, J. Kestin, ed. (AIP Conf. Proc. 11, 1973), p. 229.
48. J. V. Sengers, R. S. Basu, and J. M. H. Levelt Sengers, *NASA Contractor Report* 3424 (1981).
49. T. Ohta, *Progr. Theor. Phys.* **54**:1566 (1975).
50. T. Ohta and K. Kawasaki, *Progr. Theor. Phys.* **55**:1348 (1976).
51. J. C. Nieuwoudt and J. V. Sengers, *J. Chem. Phys.* **90**:763 (1990).
52. R. F. Berg and M. R. Moldover, *Phys. Rev.* **A42**:7183 (1990).
53. R. Krauss, J. Luettmer-Strathmann, J. V. Sengers, and K. Stephan, *Int. J. Thermophys.* **14**:951 (1993).
54. J. M. H. Levelt Sengers, W. L. Greer, and J. V. Sengers, *J. Phys. Chem. Ref. Data* **5**:1 (1976).
55. R. S. Basu and J. V. Sengers, *J. Heat Trans. Trans. ASME* **101**:3 (1979).
56. K. Ohgaki, S. Umezono, and T. Katayama, *J. Supercrit. Fluid* **3**:78 (1990).
57. G. A. Olchowy and J. V. Sengers, *Phys. Rev. Lett.* **61**:15 (1988).